Catena 235 (2024) 107679

Contents lists available at ScienceDirect

Catena

journal homepage: www.elsevier.com/locate/catena

Variation of runoff-sediment relationship at flood event scale in three typical watersheds of the Loess Plateau

Ren Geng [a], Zixuan Ye [b], Peng Tian [a,b,*], Qiu Jin [a], Bo Bi [a,*], Guangju Zhao [a,b,c], Xingmin Mu [b,c], Tongshun Wang [d], Dadong Zhu [d]

[a] State Key Laboratory of Hydrology-Water Resources and Hydraulic Engineering, Nanjing Hydraulic Research Institute, Nanjing 210029, China
[b] Institute of Soil and Water Conservation, Northwest A & F University, Yangling, Shaanxi 712100, China
[c] Institute of Soil and Water Conservation, Chinese Academy of Sciences & Ministry of Water Resources, Yangling, Shaanxi 712100, China
[d] Jiangsu Hydraulic Research Institute, Nanjing 210017, China

ARTICLE INFO

Keywords:
Loess Plateau
Flood event
Runoff-sediment relationship
Soil and water conservation measures

ABSTRACT

River runoff and sediment load are characterized by topography, climate patterns, and vegetation in the watershed. The relationship runoff and sediment load has been greatly altered in many rivers throughout the world, as well as rivers in the Chinese Loess Plateau (LP) due to large-scale ecological restoration and soil conservation measures implementation. This study attempts to identify the changes of runoff-sediment relationship in three watersheds: the Gushanchuan River watershed, Jialu River watershed and Xichuan River watershed by using the flood event data during the periods of 1974–1989 and 2007–2019 in the LP. The results indicated that both runoff depth and sediment yield of flood events during 2007–2019 reduced significantly compared with those during 1974–1989 in all the watersheds. The highest decrease was found in the Gushanchuan River watershed, exhibiting reduction of 56.48% and 95.03% in runoff and sediment yield, respectively. The ratios between sediment yield and runoff depth in all three watersheds showed significant decrease during 2007–2019 when comparing to those in 1974–1989. The correlations between runoff and sediment variables became worse in 2007–2019, compared with those during 1974–1989. The implementation of soil and water conservation (SWC) measures (vegetation restoration, terraces and check dams) accounted for the changes in runoff-sediment relationship in all three watersheds. The result of this study could provide valuable information for the influences of SWC implementation and guide soil erosion control in the LP.

1. Introduction

Riverine runoff and sediment exert great influence on the geomorphologic features of the rivers, alluvial plains and deltas, and transportation of multiple terrestrial materials for sustaining aquatic ecosystems (Curmi et al., 2013; Kondolf et al., 2014). Climate variability (i.e. global warming, rainfall fluctuation) and human activities (i.e. afforestation, dams and large reservoirs, inappropriate irrigation) have considerably altered hydrological cycles, thus leading to significant changes in runoff and sediment transport in many rivers throughout the world (Luce and Holden, 2009; Geng et al., 2022). Investigating the variation of runoff and sediment load and their driving factors is of great importance for water resources management and soil conservation measures for decision-makers (Yang et al. 2022).

Numerous researches have been carried out to assess the changes of runoff and sediment load in the past several decades (Syvitski, 2003; Walling, 2006; Borrelli et al., 2015; Kemp et al., 2020). Costa et al. (2018) analyzed the variations of suspended sediment load in a regulated Alpine catchment, and found that the dominant driving factors were erosive rainfall, ice-melt, and snowmelt. Ahn and Merwade (2014) indicated that various human activities exerted great influences on runoff rather than climate change in four American watersheds. Zhao et al. (2017a) found that intensive human activities were the primary factors that resulting in the decline of runoff and sediment yield on the Loess Plateau (LP). These studies were meaningful for understanding the variations of runoff and sediment load and potential causes.

The Yellow River (YR), which is famous for the highest sediment-laden river worldwide, is the second longest river in China (Gu et al.,

* Corresponding authors at: State Key Laboratory of Hydrology-Water Resources and Hydraulic Engineering, Nanjing Hydraulic Research Institute, Nanjing 210029, China (P. Tian and B. Bi).
E-mail addresses: pengtian@nhri.cn (P. Tian), bbi@nhri.cn (B. Bi).

https://doi.org/10.1016/j.catena.2023.107679
Received 31 August 2023; Received in revised form 28 October 2023; Accepted 5 November 2023
Available online 9 November 2023
0341-8162/© 2023 Elsevier B.V. All rights reserved.

Table 1
Abbreviations of watersheds and runoff and sediment variables.

Item	Index	Details	Units
Proper noun	LP	Chinese Loess Plateau	\
	SWC	Soil and water conservation	
	YR	Yellow River	\
	R	Pearson correlation coefficient	\
	MAT	Mean annual temperature	\
	MAP	Mean annual precipitation	\
Watersheds	GRW	Gushanchuan River watershed	\
	JRW	Jialu River watershed	\
	XRW	Xichuan River watershed	\
Time	T	Duration of a flood event	minute
Runoff	H	Total runoff volume per area of a flood event	mm
	Q_{max}	The highest flow within a flood event	$m^3\ s^{-1}$
	Q_m	The average flow of a flood event	$m^3\ s^{-1}$
Sediment	SL	Total sediment load of a flood event	t
	SSC	Suspended sediment concentration of a flood event	$kg\ m^{-3}$
	SSY	Sediment yield per unit area of a flood event	$t\ km^{-2}$
	S_{max}	The highest suspended sediment concentration of a flood event	$kg\ m^{-3}$

2019; Douglas, 1989). Changes in runoff and sediment load of the YR is closely related to the prevention of flood disaster, rational allocation of water resources, eco-environment conservation and other environment issues in the middle and lower reaches of the YR basin (Cai and Rosegrant, 2004; Liu et al., 2020). Therefore, variation in runoff and sediment load of the YR is one of the major scientific topics in the field of water science in China, which considerably influence the watershed water resources allocation, soil and water conservation (SWC) planning and hydraulic projects construction (Zhang et al., 2008).

Changes of runoff and sediment load and their relationship are synergistically influenced by natural factors and human activities such as vegetation, rainfall, land use, SWC measures, etc. (Ahn, & Merwade, 2014; Kemp et al., 2020; Wang et al., 2022). In recent decades, numerous studies have been undertaken to investigate spatial and temporal changes of runoff and sediment load and potential causes in the rivers of the LP (Rustomji et al., 2008; Liang et al., 2015). Gao et al. (2011) demonstrated that precipitation resulted in 30.5 ~ 55.6% and 5.3 ~ 25.8% of runoff and sediment decline respectively in different periods. Wang et al. (2015) analyzed runoff and sediment changes in the YR basin, and found that the principal factors leading to sediment decline from 1970s to 1990s were engineering measures, i.e. terracing, check dams and reservoirs, while it was vegetation restoration after 1990s. Gu et al. (2019) indicated that SWC measures and water extraction accounted for approximately 50% in runoff decrease and more than 70% of sediment reduction. Liu et al. (2020) reconstructed natural runoff in the middle reaches of the YR using chronology method, and their results indicated that precipitation and human activities explained the reduced runoff and sediment load. Yang et al. (2022) investigated the changes of annual runoff in 64 catchments across mainland of China, and found that vegetation restoration was closely related to the runoff variations.

Countless studies have shown that human activities, especially the implementation of SWC measures, are the main reasons for the sharp decrease of runoff and sediment in the YR basin (Wang et al., 2010; Wang et al., 2015; Xu, 2004). Extreme rainfall played a vital role in soil erosion, and yielded large proportion of soil loss on the LP (Comino et al., 2017). Duan et al. (2020) stated that the runoff coefficient and soil

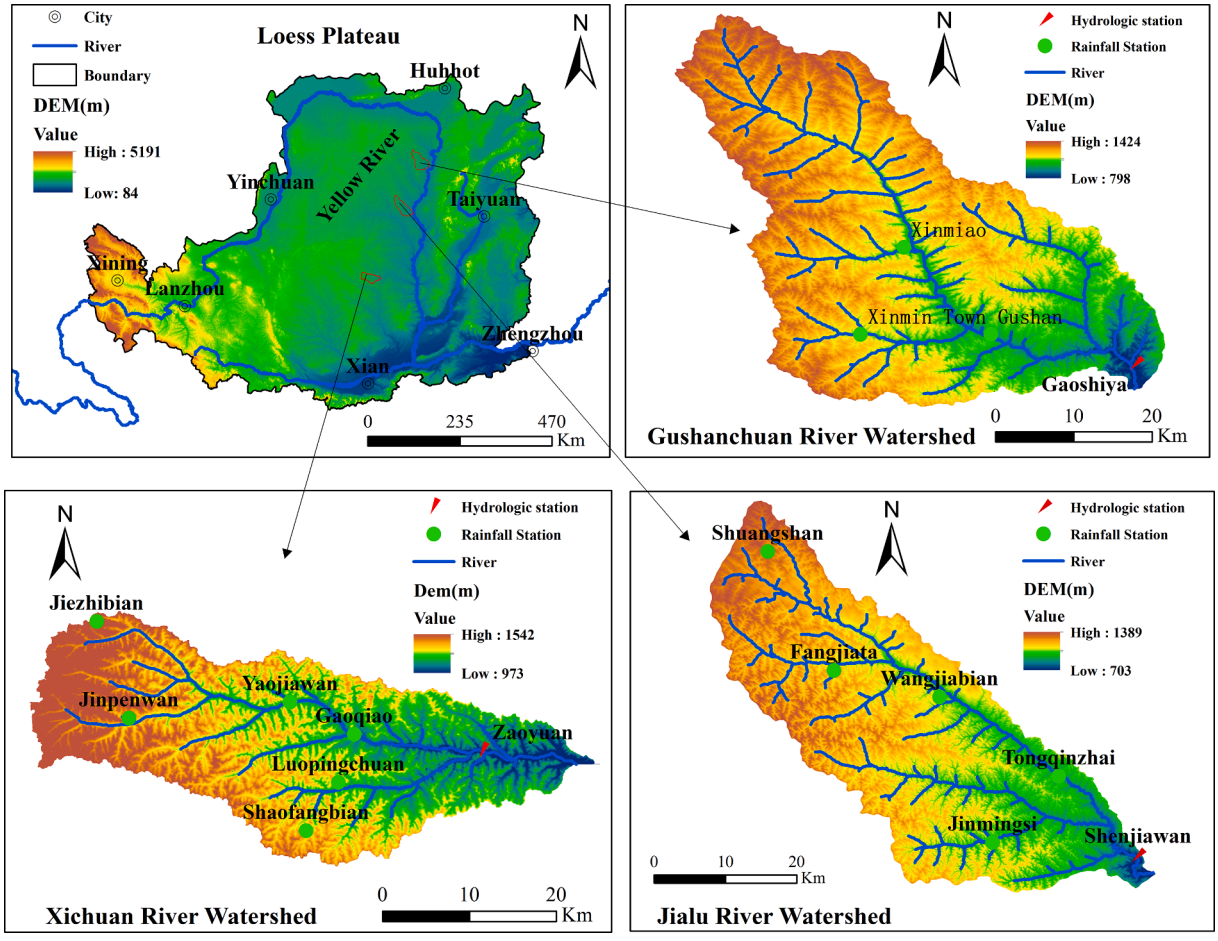


Fig. 1. The location of study area.

Table 2
Information of three watersheds.

Watersheds	Area(km^2)	River length (km)	Average annual runoff depth of flood events (mm a^{-1})		Average annual sediment yield of flood events (10^4 t a^{-1})	
			1974–1989	2007–2019	1974–1989	2007–2019
Gushanchuan River	1 273	79.4	4.54	1.98	264.99	13.16
Jialu River	1 134	93	1.73	3.39	81.08	65.42
Xichuan River	801	65.3	2.71	1.48	81.35	18.14

loss amount of extreme rainfall were 2.8 and 11.1 times greater than that of ordinary rainfall. Most of previous studies concentrated on the annual changes of runoff and sediment variations and their attribution (Wang et al., 2015), nonetheless, few studies paid attention to runoff-sediment relationship at flood event scale. Researches at flood event scale could provide better understanding the dynamic processes of runoff and sediment yield changes and their responses to underlining factors.

The LP covers an area of 64 × 10^4 km^2, and has spatial heterogeneity in both rainfall, vegetation and soil types. Furthermore, different dominant SWC measures were implemented in various watershed on the LP due to the spatial differences (Zhang et al., 2021). The objectives of this study are to: (1) investigate changes in runoff-sediment relationship in two different periods (1974–1989 and 2007–2019) at flood event scale in three typical watersheds of the LP, and (2) explore their responses to comprehensive SWC measures in the watersheds, which are characterized by different rainfall and soil types. The results of this work are expected to provide a reference for future ecological restoration and SWC in the LP.

2. Study areas

The LP covers approximately 85.06 % of the YR basin and is the primary sediment source of the YR (Table 1). Near 90% sediment of the YR come from the LP. The arid and semiarid climate zone dominate the LP, with decreased mean annual temperature (MAT) and mean annual precipitation (MAP) from south to north (Yang et al., 2019). Soil texture also become coarser from south to north. The vegetation zone changed from south forest zone to north steppe-desert zone (Geng et al., 2015). The LP is characterized of deep gullies and steep slopes, with soil erosion rates ranging from 5000 to 20000 Mg km^{-2} year^{-1} on average (Geng et al., 2017). In the study, we selected three watersheds for investigation: the Gushanchuan River watershed (GRW), Jialu River watershed (JRW) and Xichuan River watershed (XRW) in the middle reaches of the YR (Fig. 1 and Table 2), according to spatial distribution and SWC measures. The rainfall and soil texture of three watersheds become less and sander, respectively, from south (the XRW) to north (the GRW).

2.1. Gushanchuan River watershed

The Gushanchuan River is the primary tributary of the YR, located in the right bank of the middle reaches. It originates from Jungar Banner of Inner Mongolia province and eventually flows into the YR at Fugu County of Shaanxi province. The length and the drainage area of the Gushanchuan River are 79.4 km and 1273 km^2 (above Gaoshiya hydrologic station), respectively. The GRW had MAT of 7.3 °C and MAP of 410 mm. The precipitation showed great interannual variation and was characterized as short duration and high intensity storm. The geomorphological type of the watershed is the hilly and gully region on the LP, with gully density of 2.9 km km^{-2}. The average annual sediment yield was greater than 15,000 t km^{-2} year^{-1} before 1980, and contributed large proportion of sediment of the YR.

2.2. Jialu River watershed

The Jialu River is located in Jia County in northern margin of Mu Us desert and is the primary tributary of the YR. The length of the Jialu River is 93 km, with a drainage area of 1134 km^2 (above Shenjiawan hydrologic station). The JRW has the MAT of 10 °C and the MAP of 407.6 mm. The watershed belongs to the loess hilly and gully area, with gully density of 3.24 km km^{-2}. The annual average runoff and sediment yield were 58 million m^3 and 11 million tons (with annual sediment yield of 10300 t km^{-2} year^{-1}) during the period of 1957–2014, respectively. The average specific sediment yield was 10300 t km^{-2} a^{-1}.

Table 3
Frequency of flood events during study period in three watersheds.

Watersheds	1974–1989	2007–2019	Total number
Gushanchuan River	113 (7.1)	31 (2.4)	144
Jialu River	100 (6.3)	43 (3.6)	143
Xichuan	92 (5.8)	24 (1.8)	116

2.3. Xichuan River watershed

The Xichuan River is the first-order tributary of the Yanhe River, in the middle of reaches of the YR. The river length and drainage area (above Zaoyuan hydrologic station) of the Xichuan River are 65.3 km and 719 km^2. The MAT and MAP are 9.4 °C and 520.0 mm, respectively. Most of rainfall occurred in flood season (from June to September) with rainfall type of short duration and high intensity. The topography of the XRW is fragmented, with gully landforms and valley terrace. Average annual runoff and sediment load are 22.09 million m^3 and 3.19 million tons, respectively.

3. Methods and datasets

3.1. Data sources

The measured runoff and suspended sediment data at flood event scale were collected for investigation at three hydrological stations (Gaoshiya station in the GRW, Shenjiawan station in the JRW, and Zaoyuan station in the XRW) during two periods 1974–1989 and 2007–2019. In total, we collected 29 years data, which included 144 events in the GRW, 143 events in the JRW, and 116 events in the XRW (Table 3). The hydrological data at each station were obtained from the Hydrological Yearbook of the YR Basin released by the Yellow River Conservancy Commission of the Ministry of Water Resources of the People's Republic of China. Flood events were intensively sampled to obtain high temporal resolution data of the hydrological processes. Generally, the sampling interval was 6 or 12 min during floods, and then increased to 4 and 6 h for flood release period. The water level recorded by an automatic water level recorder was employed to calculate the runoff by the way of calibrated runoff water level recorder. Different intervals were used to sample water during various flood processes. Water samples were analyzed in a laboratory to obtain the suspended sediment concentration. The sediment load was calculated based on runoff, suspended sediment concentration and time interval. The national standards published by the Ministry of Water Resources was adopted to measure all the water level, runoff and suspended sediment concentration. The reliability, consistency and representativeness of the data were analyzed and verified by the hydrology department before release.

In addition, the spatial distribution of SWC measures, e.g. terraces

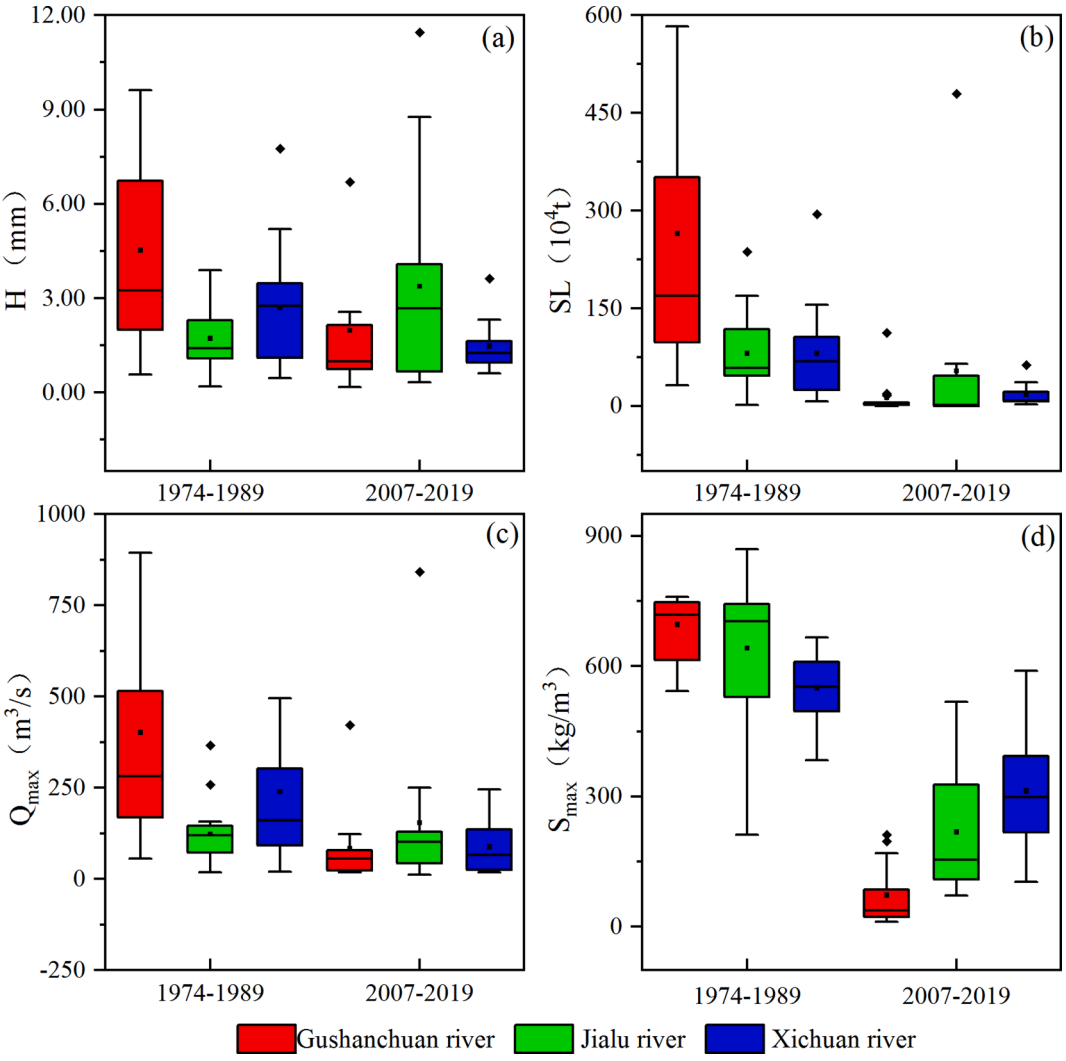


Fig. 2. Characteristics of the flood events in three watersheds during two periods.

and check dams were obtained from the Yellow River Conservancy Committee, which were obtained through field survey in 2018. The check dams data include of their numbers, location, storage capacities and construction date. The Digital Elevation Model (DEM) data of the watersheds with a resolution 30 m were downloaded from the geospatial data cloud platform (http://www.gscloud.cn). A monthly 250 m resolution NDVI (Normalized Differential Vegetation Index) MOD13A products (2000–2018) were obtained from the NASA EOS DATA Gate way (http://wist.echo.nasa.gov/api). The DEM (90 m) used in the study was derived from SRTM (Shuttle Rada Topography Mission, https://srtm.csi.cgiar.org/).

3.2. Methods

3.2.1. Flow-Sediment relationship

For a particular flood event, the total runoff volume of the event can be estimated by the following equation.

$$Q(t_1,t_2)=\int_{t_1}^{t_2} Q_t dt \tag{1}$$

And the runoff depth (H) can be estimated as:

$$\mathrm{H}(\mathrm{t}_1,\mathrm{t}_2)=\frac{\int_{t_1}^{t_2}\mathrm{Q_t dt}}{\mathrm{A}}=\frac{\sum \mathrm{Q_t}\Delta \mathrm{t}}{\mathrm{A}} \tag{2}$$

where Δt (min) is the runoff observation time at the hydrological station, the instantaneous flow is Q_t ($m^3\ s^{-1}$), and A is the drainage area (km^2).

The sediment load for flood event (SL) is calculated as:

$$\mathrm{SL}(\mathrm{t}_1,\mathrm{t}_2)=\int_{t_1}^{t_2}\mathrm{Q_t\cdot SSC_t\cdot dt}=\sum \mathrm{Q_t\cdot SSC_t.\Delta t} \tag{3}$$

and the specific sediment yield (SSY) equal to:

$$SSY=\frac{SY(t_1,t_2)_{total}}{A}=\frac{\int_{t_1}^{t_2} SSC_t\cdot Q_t dt}{A} \tag{4}$$

where SSC_t (kg m^{-3}) is the suspended sediment concentration at time t. Then the Eq(4) can be simplified as:

$$SSY=\frac{SSC\cdot\overline{Q}\Delta t}{A}+\varepsilon=SSC\cdot H+\varepsilon \tag{5}$$

where ε is the residue error.

The runoff-sediment relationship denotes the correlation between H and SSY (H-SSY) among all the flood events. According to data availability and the progresses of SWC, the collected data including two periods: 1974–1989 and 2007–2019. The former period can be regarded as the referenced period when the influences human activities were

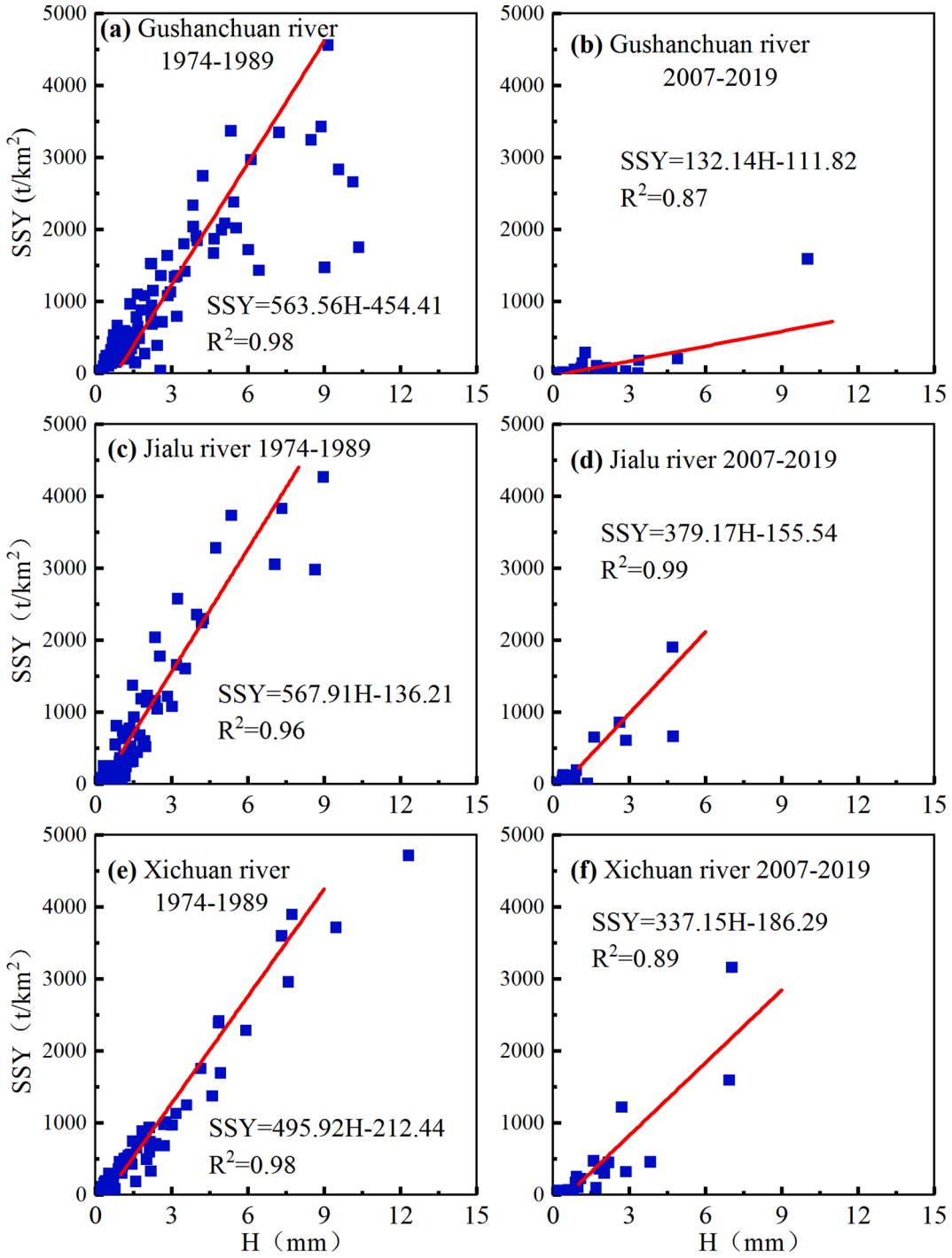


Fig. 3. The runoff and sediment relationship of flood events in three watersheds of two periods.

limited, while the latter period was the intensive human influenced period. Thus, we here applied the linear proportional relationship to detect the temporal dynamic of the relationship between H-SSY for each event during two different periods in different watersheds.

3.2.2. Correlation analysis

For a given flood event, we selected different variables (Table 1), including duration of a flood event (T), H, peak flood flow (Q_{max}), average flow (Q_m), SL, SSC and maximum sediment concentration (S_{max}) to quantify their correlation.

The correlation between runoff and sediment variables was expressed by the Pearson correlation coefficient (R). The calculation formula of R was listed as followed.

$$R = \frac{Cov(X, Y)}{\sqrt{Var[X]Var[Y]}} \quad (3)$$

Where: Cov(X, Y), Var[X] and Var[Y] were the covariance of X and Y, the variance of X and the variance of Y, respectively.

Pearson correlation analysis was conducted by ggpairs package in R 4.2.3 (https://r-charts.com/correlation/ggpairs/). SPSS (19.0) (SPSS Inc.) was applied to conduct the linear regression between variables. The figures of study area, changing slope of NDVI, terraces and check dams were drawn by Arcgis 10.8.

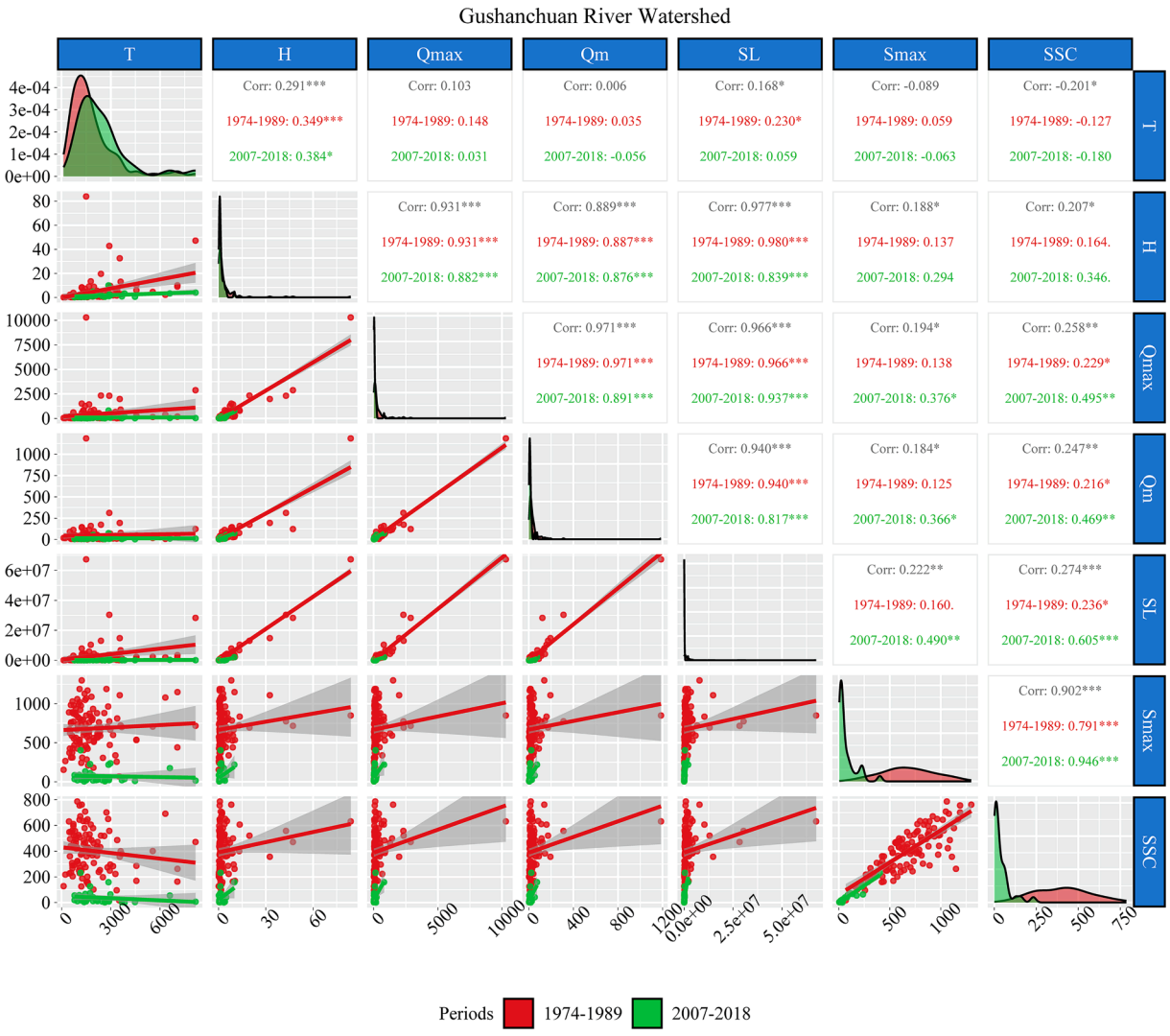


Fig. 4. Correlation analysis between runoff and sediment variables of flood events in the Gushanchuan River watershed.

4. Results

4.1. Changes in runoff-sediment characteristics of flood events

Fig. 2 showed the runoff-sediment relationship changes of flood events in each watershed in 1974–1989 and 2007–2019. Overall, the H (total runoff volume per area of a flood event), SL (total sediment load of a flood event), Q_{max} (the highest flow within a flood event) and S_{max} (the highest suspended sediment concentration of a flood event) all decreased in different degrees. The SL and S_{max} of GRW, JRW and XRW in 2007–2019 were all lower than those in 1974–1989. The SL of GRW, JRW and XRW decreased by 95.03%, 32.93%, and 77.70%, respectively. The highest decrease of SL appeared in the GRW, where SL decreased from 2.65 × 10^6 tons in 1974–1989 to 1.32 × 10^6 tons in 2007–2019. The S_{max} of three watersheds decreased by 89.49%, 65.96%, and 43.10%, respectively. The H of GRW and XRW decreased from 4.55 mm and 2.71 mm in 1974–1989 to 1.98 mm and 1.48 mm in 2007–2019, respectively, and the Q_{max} decreased by 79.05 % and 63.04 %, respectively. In contrast, the H and Q_{max} in the JRW increased by 1.95 and 1.25 times during 2007–2019, compared to 1974–1989. The Q_{max} and S_{max} reduced significantly in the later period, indicating that SWC measures were effective to reduce soil erosion. The H and SL decreased significantly, and SL reduced greater than H, indicating the comprehensive management of SWC of the LP exerted stronger influences on SL than H. The GRW has a larger variation of runoff and sediment variables than JWR and XRW, and different runoff and sediment variables fluctuated greatly. It was found that H, Q_{max}, SL and S_{max} in the GRW were the largest in 1974–1989 and the smallest in 2007–2019.

4.2. Changes in runoff-sediment relationship of flood events

Table 3 showed statistics of flood events in the three watersheds of 1974–1989 and 2007–2019, including 144 flood events in the GRW, 143 in the JRW, and 116 in the XRW. Both the total number and annual average number of flood events reduced significantly in the latter period. The total number of flood events in the GRW, JRW and XRWs decreased by 72.57%, 57.00% and 34.29 %, respectively, and the annual average number of flood events decreased by 66.24 %, 47.08 % and 19.12 %, correspondingly.

The H-SSY all had good linear relationships in three watersheds from 1974 to 1989, with determination coefficients higher than 0.9 (Fig. 3). The best linear fitting appeared in the XRW. In the latter period, the H-SSY relationships became worse, and the determination coefficient changed to 0.87, 0.99 and 0.89 in 2007–2019, respectively.

The first-order term (slope) of the H-SSY linear regression equation denoted the sediment yield per unit runoff depth of the flood events, i.e., the SSC of all flood events. The slopes of H-SSY relationship in all three watersheds in 2007–2019, decreased significantly by 76.55%, 33.23%,



Fig. 5. Correlation analysis between runoff and sediment variables of flood events in the Jialu River watershed.

and 32.02% compared with 1974–1989, respectively. The largest decrease appeared in the GRW, with the first order reduced from 563.56 in 1974–1989 to 132.14 in 2007–2019. Similarly, it decreased from 567.91 in 1974–1989 to 379.17 in 2007–2019 in the JRW. This implied that the runoff-sediment relationship of flood events has been altered, and the sediment transport capacity of runoff has decreased due to the influences of various SWC measures. In contrast, the JRW has the highest slopes of 567.91 and 379.17 for two periods, respectively, which indicated the most serious soil erosion and sediment yield among the three watersheds.

4.3. Relationships between runoff and sediment variables of flood events

The Pearson correlation analysis (Fig. 4) indicated that H, Q_{max} and Q_m were high positively correlated to SL ($p < 0.01$), with R of 0.98, 0.97 and 0.94, respectively in the GRW in 1974–1989. The H and SL had the highest R, which implied that the intensity of erosional sediment yield during the flood events was highly related to H. The correlation between SL and each runoff variable decreased in 2007–2019. The greatest change was the correlation between SL and H, with R decreasing from 0.98 during 1974–1989 to 0.84 during 2007–2019. The Q_{max} of the runoff variables was significantly related to Q_m and H in 1974–1989, with R of 0.97 and 0.93, respectively. The correlations between the variables reflecting runoff characteristics in 2007–2019 were not significantly different from these in 1974–1989.

Fig. 5 presented the correlation analysis of runoff and sediment variables in the JRW. The H, Q_{max} and Q_m in 1974 to 1989 were positively correlated with SL ($p < 0.01$), with the R of 0.95, 0.83 and 0.84, respectively. The highest R (greater than 0.9) was examined between H and SL. This demonstrated that the sediment yield was highly correlated to H during flood events in the JRW. The correlation between SL and Q_m decreased from 0.95 within 1974–1989 to 0.66 within 2007–2019. The R among runoff variables were all above 0.80 during 1974–1989. The correlations among the runoff variables in 2007–2019 were not significantly different from those in 1974–1989.

As Fig. 6 shown, the H, Q_{max} and Q_m showed significantly positive correlations ($p < 0.01$) with SL during 1974–1989, with R of 0.98, 0.93 and 0.92, respectively in the XRW. The R of H and SL were above 0.95, indicating that the erosional sediment yield of flood events was more closely related to H in the XRW. The correlation between SL and other variables weakened in 2007–2019. The R of between SL and H, Q_{max} and Q_m decreased to 0.84, 0.77 and 0.88 in 2007–2019, respectively. Among the runoff variables, The H was closely related to Q_{max} and Q_m, with R of 0.88 and 0.92 during 1974–1989, correspondingly. For the period of 2007–2019, the correlation between H, and Q_m and Q_{max} declined. The R decreased from 0.88 and 0.92 of 1974–1989 to 0.65 and 0.79 of 2007–2019, respectively.

The SSC and S_{max} were significantly correlated among the sediment



Fig. 6. Correlation analysis between runoff and sediment variables of flood events in the Xichuan River watershed.

variables of flood events in the GRW, JRW and XRW. The correlations among the sediment variables during 2007–2019 were not significantly different from these during 1974–1989. There existed no significant relationship between the flood period (T) and runoff variables (H, Q_{max}, and Q_m) and sediment variables (SL, S_{max} and SSC) of both periods in each watershed.

5. Discussion

5.1. Changes in runoff and sediment variables of flood events and their correlations

When comparing runoff and sediment of flood events in the two periods, the H, Q_{max}, SL and S_{max} were much lower during the period of 2007–2019 than those in 1974–1989 in the GRW and XRW. The significant decrease of runoff and sediment in the two watersheds was in agreement with the finding of other watersheds on the LP (Liu et al., 2013). Tian et al. (2016) investigated dynamics of runoff and sediment in the Beiluo River watershed. They found significantly decrease in both runoff and sediment between 1979 and 1999, which could be attributed to the implementation of SWC measures. The SL and S_{max} showed similar decrease in the JRW. Overall, large scale of SWC measures (vegetation restoration, terraces and check dams) are responsible for the reduction of soil detachment capacity and sediment transport capacity in the watersheds (Demissie et al., 2015). Nevertheless, the H and Q_{max} increased in the JRW, which was different from the GRW and XRW. The increased H and Q_{max} could be explained by the increasing extreme rainfall in the later watershed period (Zhai et al., 2021).

The GRW showed the highest decrease in runoff and sediment variables among three watersheds in two periods. This finding can be attributed to the greatest improvement of vegetation coverage from 13.6% in 1980s to nearly 60% in 2020 in the GRW (Mu et al., 2007; Tian et al., 2022). The SWC measures, especially the extensive vegetation restoration, are the principal reason for the reduction of runoff and sediment in the LP (Feng et al., 2016; Liu et al., 2014). In contrast, we found that runoff and sediment variable had gentle decline in the JRW, which was due to the low vegetation coverage and increase of storm events (Lian et al., 2020; Zhai et al., 2021).

The slopes of the H-SSY decreased significantly in all watersheds after the implementation of SWC measures. Similar findings were examined by Zhao et al. (2017b), which compared the relationship in the Huangfuchuan watershed and Yanhe watershed on the LP. Apparently, the decreased slope of the H-SSY was largely related to intensive anthropogenic activities (vegetation restoration, land use changes and etc.) (Tian et al., 2022). The linear regression slope of the GRW demonstrated the largest decline among three watersheds, which was similar to the changes of runoff and sediment variables. The slopes of linear regression model of three watersheds showed different degree of

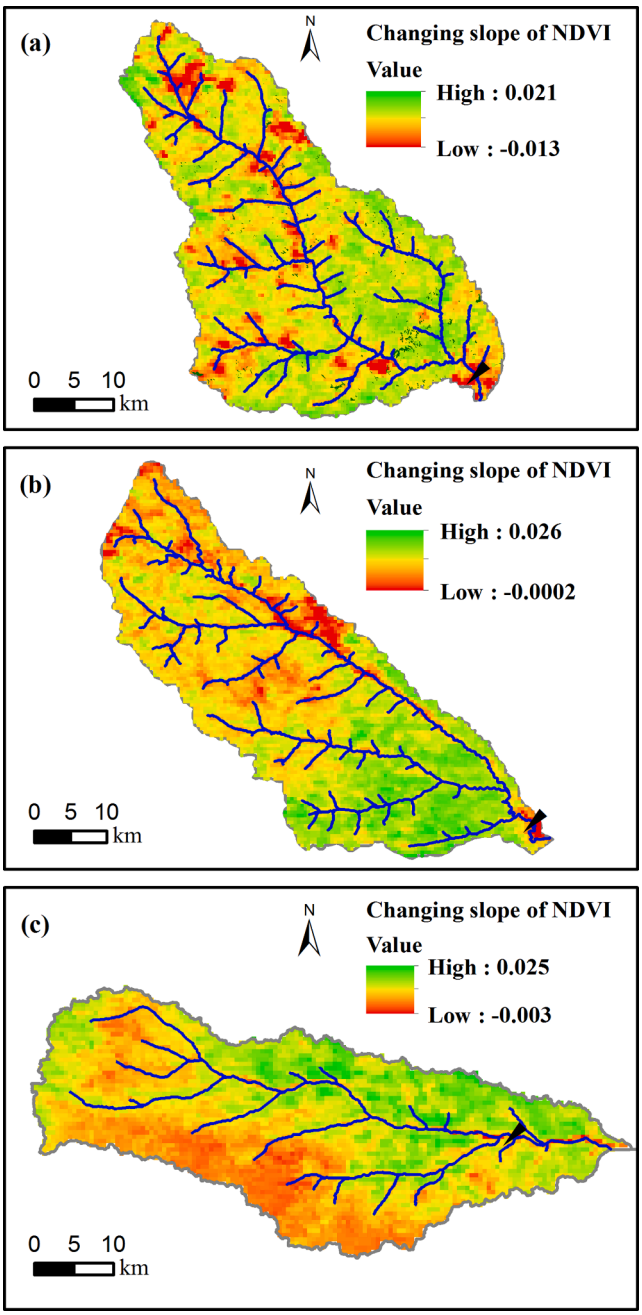


Fig. 7. The changing slope of NDVI (2000–2018) in the Gushanchuan River watershed (a), Jialu River watershed (b) and Xichuan River watershed (c).

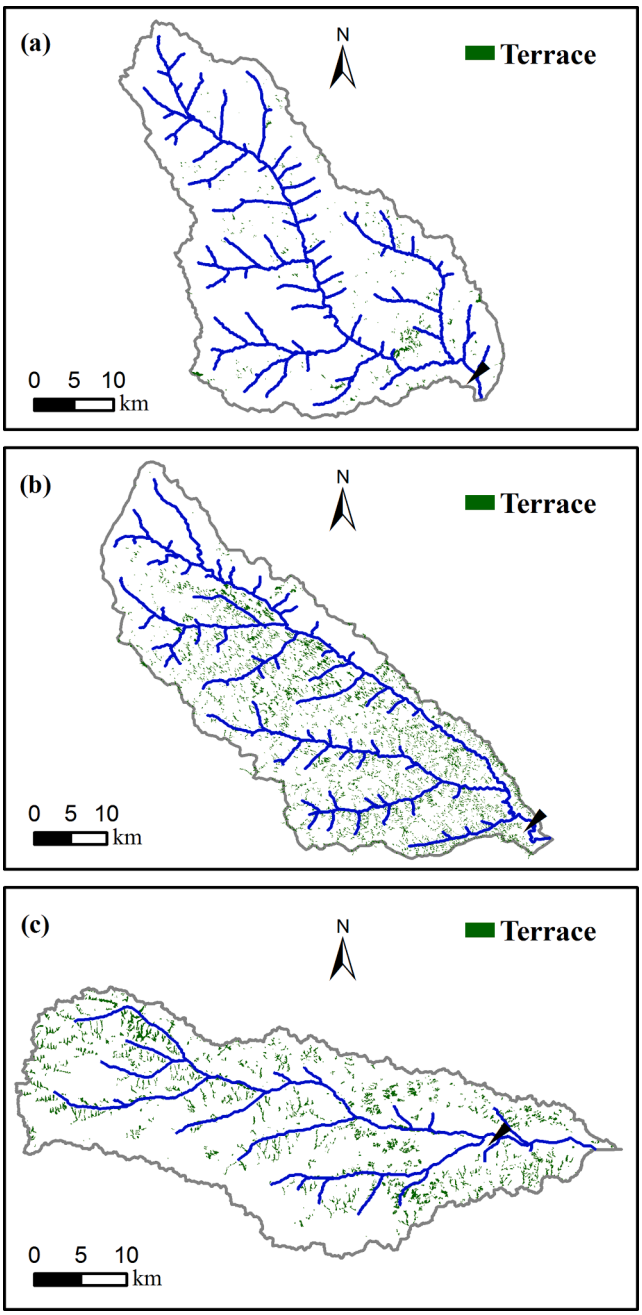


Fig. 8. Terraces (2000–2018) in the Gushanchuan River watershed (a), Jialu River watershed (b) and Xichuan River watershed (c).

decrease, which were mainly attributed to the differences of erosional agents, storm events and SWC measures in three watersheds (Geng et al., 2015; Hu et al., 2022).

5.2. *Influence of SWC measures on runoff and sediment changes*

Since 1950s, SWC measures have been carried out to reduce soil erosion on the LP. From 1950s to 1970s, the effects of SWC measures on runoff and sediment load were relatively limited since their total amounts were small (Zhao et al., 2017b). Afterwards, the LP has undergone large-scale conservation management. Especially after 1999, vegetation cover improved greatly due to the implementation of "Green for Grain" project. The implementation of SWC measures which effectively reduced soil erosion on the slope and the amount of sediment yield on the LP (Wang et al., 2014; Zheng, 2018). Wang et al. (2015) indicated vegetation restoration, terrace farming, and check dams and reservoirs accounted for 10%, 33% and 21% of sediment reduction, respectively.

Large-scale vegetation restoration in the LP has significantly changed the subsurface environment, which results in the increase of rainfall retention and infiltration (Wang et al., 2015). The increase of surface roughness, induced by vegetation restoration, contributed to the decrease of hydrodynamic force, soil detachment capacity and sediment transport capacity (Li and Pan, 2018; Geng et al., 2021). As shown in Fig. 7, most parts of three watershed showed increasing trend of NDVI. For example, the vegetation coverage of the JRW increased 27.33 % (1989) to 50.4 % (2012) (Lian et al., 2020). The grassland and forest coverage of the XRW had increased from 33.09% in 1980 to 63.00% in 2012. The great improvement of vegetation coverage of three watersheds played a vital role in the reduction of runoff and sediment load (Feng et al., 2016).

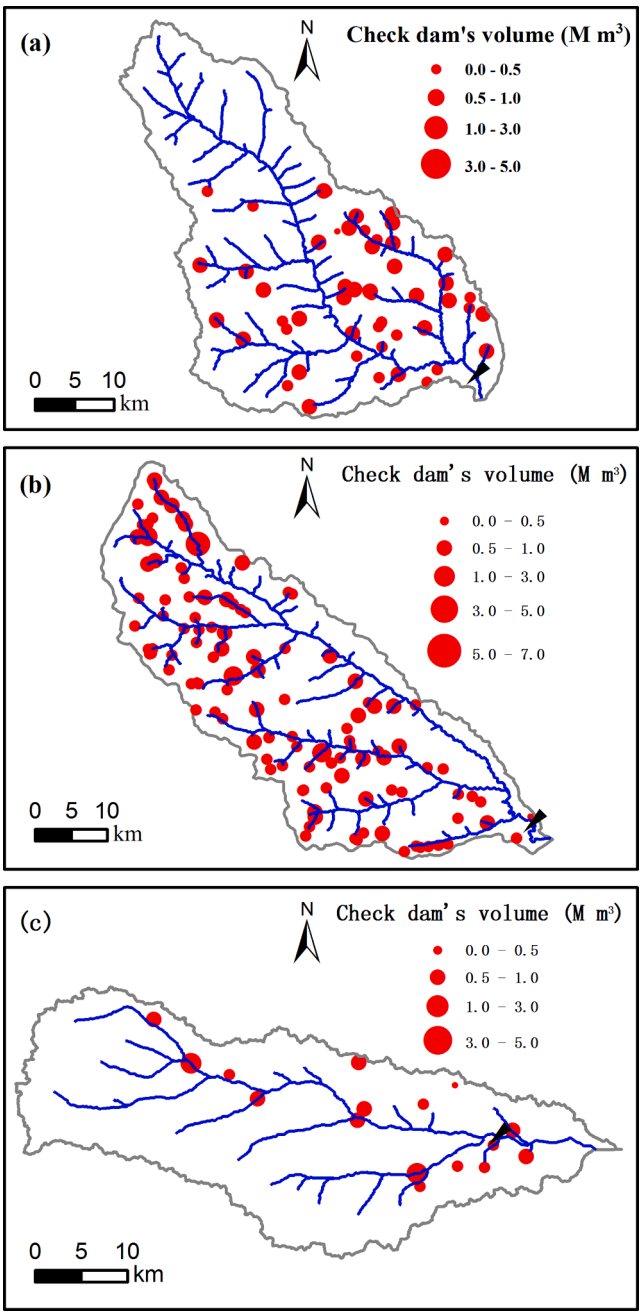


Fig. 9. Check dams distribution in the (a) Gushanchuan River watershed, (b) Jialu River watershed and (c) Xichuan River watershed.

Terraces reshape the micro-topography and increase the slope length, which intercept flow pathways on hillslope (Tarolli et al., 2014). Terraces intercept runoff produced by themselves or by upstream incoming runoff (Hu et al., 2022). Hu et al. (2022) stated that terraces were responsible for 9.9%-43.8% of the sediment variation for three watersheds on the LP. The implemented terraces areas of the GRW, JRW and XRW were 40 km^2, 24.17 km^2 and 53.69 km^2, respectively, by the end of 2018 (Fig. 8). The implementation of terraces explained the decreased runoff and sediment load of three watersheds (Hu et al., 2022).

Check dams are the vital engineering conservation measures, and could retain flood water, trap incoming sediment, increase valuable water for agriculture production and reduce downstream sediment transport (Ferrazzi and Botter, 2019). Zhang et al. (2021) assessed changes in streamflow regimes in three watersheds on the LP and found that check dams increased the seepage of soil water and decreased extreme high flow. By the end of 2018, there have been 55, 117 and 16 check dams constructed in the GRW, JRW and XRW, which cumulatively trapped 41.02, 98.49 and 15.15 M m^3 sediment. As shown in Fig. 9, though relative higher check dams were builded in the JRW, the runoff and sediment load showed insignificant reduction due to increasing storm events.

6. Conclusions

This study selected three watersheds to analyze the changes of runoff and sediment loads and their relationship during the periods of 1974–1989 and 2007–2019 at flood event scale. The major conclusions can be summarized as follows.

The H, Q_{max}, SL and S_{max} of flood events during 2007–2019 were significantly lower than those of 1974–1989 in the GRW and XRW. Nevertheless, the changing trends of runoff and sediment variables in JRW were not obvious. The slopes of the H-SSY of the GRW, JRW and XRW in 2007–2019 decreased significantly compared with 1974–1989. The significant decreases of runoff and sediment variables and slopes of H-SSY were attributed to the implementation of SWC measures. The GRW had the greatest decreases of runoff and sediment variables and slope of linear regression, which could be explained by the significant improvement of vegetation coverage in this watershed. The correlation between the SL and runoff variables (H, Q_{max}, Q_m) weaken due to various human activities, especially the SWC measures in all the watersheds. The sediment concentration decreased with H and Q_{max}, indicating less amount of hyper-concentrated flow events, which resulted in less sediment discharged into the YR.

This study explored the related variables of runoff and sediment in the three watersheds and discussed influencing factors of the variations of runoff and sediment. The results of this study were meaningful for the implementation of SWC measures in the LP and other places in the world. Further studies should be conducted to investigate how vegetation restoration, terraces and check dams influence the runoff and sediment yield in the watersheds.

Declaration of Competing Interest

The authors declare that they have no known competing financial interests or personal relationships that could have appeared to influence the work reported in this paper.

Data availability

Data will be made available on request.

Acknowledgement

This study was financially supported by the National Natural Science Foundation of China (U2243211, 42077076, 42177323) and the Research Foundation of Nanjing Hydraulic Research Institute (Y922001, Y923005). The Hydrological Bureau of the Yellow River Conservancy Commission was also appreciated for providing hydrological data.

References

Ahn, K.H., Merwade, V., 2014. Quantifying the relative impact of climate and human activities on streamflow. J. Hydrol. 515, 257–266.
Borrelli, P., Märker, M., Schütt, B., 2015. Modelling post-tree-harvesting soil erosion and sediment deposition potential in the Turano River Basin (Italian Central Apennine). Land Degrad. Dev. 26 (4), 356–366.
Cai, X., Rosegrant, M.W., 2004. Optional water development strategies for the Yellow River Basin: Balancing agricultural and ecological water demands. Water Resour. Res. 40 (8), W08S04.
Comino, J.R., Senciales, J.M., Ramos, M.A., Martínez-Casasnovas, J.A., Lasanta, T., Brevik, E.C., Ries, J.B., Sinoga, J.R., 2017. Understanding soil erosion processes in Mediterranean sloping vineyards (Montes de Málaga, Spain). Geoderma 296, 47–59.

Costa, A., Anghileri, D., Molnar, P., 2018. Hydroclimatic control on suspended sediment dynamics of a regulated Alpine catchment: a conceptual approach. Hydrol. Earth Syst. Sci. 22 (6), 3421–3434.
Curmi, E., Richards, K., Fenner, R., Allwood, J.M., Kopec, G.M., Bajželj, B., 2013. An integrated representation of the services provided by global water resources. J. Environ. Manage. 129, 456–462.
Demissie, B., Frankl, A., Haile, M., Nyssen, J., 2015. Biophysical controlling factors in upper catchments and braided rivers in drylands: the case of a marginal graben of the Ethiopian Rift valley. Land Degrad. Dev. 26 (7), 748–758.
Douglas, I., 1989. Land degradation, soil conservation and the sediment load of the Yellow River, China: review and assessment. Land Degrad. Dev. 1 (2), 141–151.
Duan, J., Liu, Y.J., Yang, J., Tang, C.J., Shi, Z.H., 2020. Role of groundcover management in controlling soil erosion under extreme rainfall in citrus orchards of southern China. J. Hydrol. 582, 124290.
Feng, X., Fu, B., Piao, S., Wang, S., Ciais, P., Zeng, Z., Liu, Y.H., Zeng, Y., Li, Y., Jiang, X. H., Wu, B., 2016. Revegetation in China's Loess Plateau is approaching sustainable water resource limits. Nature Clim. Change 6 (11), 1019–1022.
Ferrazzi, M., Botter, G., 2019. Contrasting signatures of distinct human water uses in regulated flow regimes. Environ. Res. Commun. 1 (7), 071003.
Gao, P., Mu, X.M., Wang, F., Li, R., 2011. Changes in streamflow and sediment discharge and the response to human activities in the middle reaches of the Yellow River. Hydrol. Earth Syst Sci. 15 (1), 1–10.
Geng, R., Zhang, G.H., Li, Z.W., Wang, H., 2015. Spatial variation in soil resistance to flowing water erosion along a regional transect in the Loess Plateau. Earth Surf. Proc. Land. 40 (15), 2049–2058.
Geng, R., Zhang, G.H., Ma, Q.H., Wang, H., 2017. Effects of landscape positions on soil resistance to rill erosion in a small catchment on the Loess Plateau. Biosys. Eng. 160, 95–108.
Geng, R., Zhang, G.H., Hong, D.L., Ma, Q.H., Jin, Q., Shi, Y.Z., 2021. Response of soil detachment capacity to landscape positions in hilly and gully regions of the Loess Plateau. Catena 196, 104852.
Geng, R., Jin, Q., Lei, S., Liu, H., Lu, B., Xie, M., 2022. Comparison of Critical Shear Stress of Rill Erosion Estimated from Two Methods. Water 14 (12), 1949.
Gu, C., Mu, X., Gao, P., Zhao, G., Sun, W., 2019. Changes in run-off and sediment load in the three parts of the Yellow River basin, in response to climate change and human activities. Hydrol. Process. 33 (4), 585–601.
Hu, J., Li, P., Zhao, G., Mu, X., Hörmann, G., Gao, P., Sun, W.Y., Zhang, L., 2022. Effects of climate variability and anthropogenic factors on sediment load reduction in the Weihe River basin, China. Hydrol. Process. 36 (4), e14562.
Kemp, D.B., Sadler, P.M., Vanacker, V., 2020. The human impact on North American erosion, sediment transfer, and storage in a geologic context. Nat. Commun. 11 (1), 1–9.
Kondolf, G.M., Gao, Y.X., Annandale, G.W., Morris, G.L., Jiang, E.H., Zhang, J.H., Cao, Y. T., Carling, P., Fu, K.D., Guo, Q.C., Hotchkiss, R., Peteuil, C., Sumi, T., Wang, H.W., Wang, Z.M., Wei, Z.L., Wu, B.S., Wu, C.P., Yang, C.T., 2014. Sustainable sediment management in reservoirs and regulated rivers: Experiences from five continents. Earths Future 2 (5), 256–280.
Li, C., Pan, C., 2018. The relative importance of different grass components in controlling runoff and erosion on a hillslope under simulated rainfall. J. Hydrol. 558, 90–103.
Lian, Q.H., Tian, P., Zhao, G.J., Mu, X.M., Hu, J.F., Jiang, H.X., 2020. Change of the runoff-sediment relationship and its response to ecological management in Jialu River Basin. Sci. Soil Water Conser. 18 (4), 53–61 in Chinese.
Liang, W., Bai, D., Wang, F., Fu, B., Yan, J., Wang, S., Yang, Y.T., Long, D., Feng, M.Q., 2015. Quantifying the impacts of climate change and ecological restoration on streamflow changes based on a Budyko hydrological model in China's Loess Plateau. Water Resour. Res. 51 (8), 6500–6519.
Liu, Y., Song, H., An, Z., Sun, C., Trouet, V., Cai, Q., Liu, R.S., Leavitt, S.W., Song, Y., Li, Q., Fang, C.X., Zhou, W.J., Yang, Y.K., Zhao, J., Wang, Y.Q., Sun, J.Y., Mu, X.M., Lei, Y., Wang, L., Li, X.X., Ren, M., Cui, L.L., Zeng, X., 2020. Recent anthropogenic curtailing of Yellow River runoff and sediment load is unprecedented over the past 500 y. roc. Natl. Acad. Sci. U.S.A. 117 (31), 18251–18257.
Liu, X.Y., Yang, S.T., Wang, F.G., He, X.Z., Ma, H.B., Luo, Y., 2014. Analysis on sediment yield reduced by current terrace and shrubs-herbs-arbor vegetation in the Loess Plateau. J. Hydraul. Eng. 45, 1293–1300.
Liu, E.J., Zhang, X.P., Xie, M.L., Chen, N., 2013. Change in runoff and sediment in the upper catchment of Beiluo River under the vegetation restoration. Sci Soil Water Conserv 11 (1), 39–45.
Luce, C.H., Holden, Z.A., 2009. Declining annual streamflow distributions in the Pacific Northwest United States, 1948–2006. Geophys. Res. Lett. 36 (16), L16401.
Mu, X., Zhang, L., McVicar, T.R., Chille, B., Gau, P., 2007. Analysis of the impact of conservation measures on stream flow regime in catchments of the Loess Plateau, China. Hydrol. Process. 21 (16), 2124–2134.
Rustomji, P., Zhang, X.P., Hairsine, P.B., Zhang, L., Zhao, J., 2008. River sediment load and concentration responses to changes in hydrology and catchment management in the Loess Plateau region of China. Water Resour. Res. 44 (7), W00a04.
Syvitski, J.P., 2003. Supply and flux of sediment along hydrological pathways: research for the 21st century. Glob. Planet. Change 39 (1–2), 1–11.
Tarolli, P., Preti, F., Romano, N., 2014. Terraced landscapes: From an old best practice to a potential hazard for soil degradation due to land abandonment. Anthropocene 6, 10–25.
Tian, P., Zhai, J., Zhao, G., Mu, X., 2016. Dynamics of runoff and suspended sediment transport in a highly erodible catchment on the Chinese Loess Plateau. Land Degrad. Dev. 27 (3), 839–850.
Tian, P., Feng, J., Zhao, G., Gao, P., Sun, W., Hörmann, G., Mu, X., 2022. Rainfall, runoff, and suspended sediment dynamics at the flood event scale in a Loess Plateau watershed, China. Hydrol. Process. 36 (2), e14486.
Walling, D.E., 2006. Human impact on land–ocean sediment transfer by the world's rivers. Geomorphology 79 (3–4), 192–216.
Wang, H., Bi, N., Saito, Y., Wang, Y., Sun, X., Zhang, J., Yang, Z., 2010. Recent changes in sediment delivery by the Huanghe (Yellow River) to the sea: Causes and environmental implications in its estuary. J. Hydrol. 391 (3–4), 302–313.
Wang, S., Fu, B., Piao, S., Lü, Y., Ciais, P., Feng, X., Wang, Y., 2015. Reduced sediment transport in the Yellow River due to anthropogenic changes. Nat. Geosci. 9 (1), 38–41.
Wang, Z., Xu, M., Liu, X., Singh, D.K., Fu, X., 2022. Quantifying the impact of climate change and anthropogenic activities on runoff and sediment load reduction in a typical Loess Plateau watershed. J. Hydrol. 39, 100992.
Wang, B., Zhang, G.H., Shi, Y.Y., Zhang, X.C., 2014. Soil detachment by overland flow under different vegetation restoration models in the Loess Plateau of China. Catena 116, 51–59.
Xu, J.X., 2004. Effect of human activities on overall trend of sedimentation in the lower Yellow River, China. Environ. Manage. 33 (5), 637–653.
Yang, Y., Jia, X., Wendroth, O., Liu, B., Shi, Y., Huang, T., Bai, X., 2019. Noise-assisted multivariate empirical mode decomposition of saturated hydraulic conductivity along a south-north transect across the Loess Plateau of China. Soil Soil Sci. Soc. Am. J. 83 (2), 311–323.
Yang, L., Zhao, G., Tian, P., Mu, X., Tian, X., Feng, J., Bai, Y., 2022. Runoff changes in the major river basins of China and their responses to potential driving forces. J. Hydrol. 607, 127536.
Zhai, T.T., Zhao, G.J., Mu, X.M., Gao, P., 2021. Processes of water and sediment in the representative catchments of the middle Yellow River under extreme rainfalls. J. Sediment Res. 46 (1), 57–63 in Chinese.
Zhang, X., Zhang, L., Zhao, J., Rustomji, P., Hairsine, P., 2008. Responses of streamflow to changes in climate and land use/cover in the Loess Plateau, China. Water Resour. Res. 44 (7).
Zhang, S., Zhao, G., Mu, X., Tian, P., Gao, P., Sun, W., 2021. Changes in streamflow regimes and their responses to different soil and water conservation measures in the Loess Plateau watersheds, China. Hydrol. Process. 35 (10), e14401.
Zhao, G., Mu, X., Jiao, J., An, Z., Klik, A., Wang, F., Jiao, F., Yue, X.L., Gao, P., Sun, W., 2017a. Evidence and causes of spatiotemporal changes in runoff and sediment yield on the Chinese Loess Plateau. Land Degrad. Dev. 28 (2), 579–590.
Zhao, G., Yue, X., Tian, P., Mu, X., Xu, W., Wang, F., Gao, P., Sun, W., 2017b. Comparison of the suspended sediment dynamics in two Loess Plateau catchments, China. Land Degrad. Dev. 28 (4), 1398–1411.
Zheng, M., 2018. A spatially invariant sediment rating curve and its temporal change following watershed management in the Chinese Loess Plateau. Sci. Total Environ. 630, 1453–1463.